Entropy generation optimization and activation energy in flow of Walters-B nanomaterial

Sumaira Jabeen [a,*] Tasawar Hayat [a,b] and Ahmed Alsaedi [b]

[a] Department of Mathematics, Quaid-I-Azam University 45320, Islamabad 44000, Pakistan

[b] Nonlinear Analysis and Applied Mathematics (NAAM) Research Group, Department of Mathematics, Faculty of Science, King Abdulaziz University, Jeddah 21589, Saudi Arabia

Abstract: Entropy generation in flow of Walters-B nanomaterial is addressed. Energy equation consist of ohmic heating, radiation and heat generation. Binary chemical reaction with modified Arrhenius energy is employed. The consequences of thermophoresis, Brownian motion and viscous dissipation are accounted. Convergent solutions by homotopy analysis technique are constructed. Intervals of convergence are explicitly identified. Results of physical quantities of interest are analyzed. A decrement in rate of mass transfer is noticed for higher chemical reaction parameter. Enhancing values of Brinkman number and magnetic parameter leads an increment in total entropy rate.

Keywords: Viscous dissipation; Walters-B nanofluid; Entropy generation; Thermal radiation; Heat generation/absorption; Activation energy.

1. Introduction

Extensive applications of nanotechnology in class of thermal engineering give rise to a new branch of heat transfer fluids termed as nanofluids. In formation of nanofluid, the fibers, solid particles or tubes (having length of order 1-50 nm) are dispersed in heat transfer materials like oil, water and ethylene glycol. These materials are considered as base fluids. Because of small size and mostly larger surface area of particles. The nanofluids possess novel properties including higher thermal conductivity, negligible blockage in flow channels, homogeneity and log-term constancy. Nanofluids are useful in microelectronics, automotive, power stations, fuel chambers, pharmacological methods, hybrid electric engines, cooling engine automobile, caloric controlling, local refrigerator, in crushing process, mining and boiler gas outlet, temperature control and in nuclear process. Nanomaterials acquire a special auditory characteristic that's convenient in ultrasonic demonstration. Additional influence includes shear transformation of an instant compression ray and this property becomes more operative as concentration enhances. Information of rheological implementation of nanofluids is more influential in view of their stability for convection applications. Pioneering work on nanofluid was done by Choi [1]. Recently Waini et al. [2] studied the hybrid nanomaterial flow and heat mechanism over a nonlinear porous surface. Some studies for flow of nanofluids can be consulted through the attempts [3-11].

In thermodynamics the entropy of any system is defined as the quantity of inaccessible energy. It corresponds to the irreversibility in studied system which is mainly used in thermodynamically design setups. Higher entropy loss consumes energy and influence the efficiency of system. Entropy defines the way according to which physical quantities easily separated from its constituents. When thermal energy is supplied to the system then internal energy increases and as a result thermal entropy of system enhances. Irreversible processes are defined as the systems in which surroundings of related system are not able to reach at its initial state. Entropy also defines about the consumption of energy in a system. System changes due to gradient.

*Corresponding author Tel.: + 92 51 90642172.
Email address: sumaira.jabeen@math.qau.edu.pk

It sometimes refers as temperature gradient that represents energy transfer or may be a concentration gradient which indicates mass transfer. Gradient mostly causes irreversibility within a system. Since entropy relates to the disorderedness of the system due to which energy decreased and lead to decrease in potential of work. Pioneering work on this phenomenon is done by Bejan [12]. Later he discussed entropy generation in process of heat loss during motion of fluid [13]. Several researchers now analyzed this mechanism under assumptions. Recently Liu et al. [14] examined irreversibility within curved channel in EMHD flow. Dissipative flow of Williamson fluid by rotating disk with entropy generation is analyzed by Qayyum et al. [15]. Akbarzadeh et al. [16] explained irreversibilities in a turbulent nanofluid flow by considering solar stoves through crenelated absorber plates. Bizhaem et al. [17] deliberated heat exchange and irrversibilities of flow in helical tube. Recent progress about this topic may be mentioned through the attempts [18-21].

Main theme of present research is to address entropy generation and activation energy in flow of nanomaterial. Constitutive expression of Walter-B liquid is employed in modeling. Joule heating, radiation and heat generation/absorption in energy expression are present. Total entropy rate and Bejan number are formulated. The modeled mathematical problems are computed for the convergent series solution. Homotopic procedure [22-35] is adopted for development of solutions. Discussion and conclusions are organized for physical quantities of interest against the sundry variables entering into present analysis.

2. Modeling

Irreversibility process and activation energy with binary chemical reaction in flow of Walters-B nanomaterial bounded by a stretching surface is addressed. An incompressible liquid is conducting in presence of magnetic field with constant strength B_0. Small magnetic Reynolds number leads to omission of induced magnetic field. Here x and $y-$axes are parallel and normal to the surface. Heat source/ sink is considered. Surface temperature and concentration are taken as $\tilde{T}_w$ and $\tilde{C}_w$ while ambient temperature and concentration are denoted by $\tilde{T}_\infty$ and $\tilde{C}_\infty$. Fig. 1 describes the problem geometry. Governing mathematical equations of the system are as follow [8, 26, 32]

Figure 1

$$\frac{\partial \tilde{u}}{\partial x}+\frac{\partial \tilde{v}}{\partial y}=0, \tag{1}$$

$$\tilde{u}\frac{\partial \tilde{u}}{\partial x}+\tilde{v}\frac{\partial \tilde{u}}{\partial y}=\upsilon\frac{\partial^2 \tilde{u}}{\partial y^2}-\frac{k_0}{\rho}\left(\tilde{u}\frac{\partial^3 \tilde{u}}{\partial x\partial y^2}+\frac{\partial \tilde{u}}{\partial x}\frac{\partial^2 \tilde{u}}{\partial y^2}+\tilde{v}\frac{\partial^3 \tilde{u}}{\partial y^3}-\frac{\partial \tilde{u}}{\partial y}\frac{\partial^2 \tilde{u}}{\partial x\partial y}\right)-\frac{\tilde{\sigma}B_0^2}{\rho}\tilde{u}, \tag{2}$$

$$\tilde{u}\frac{\partial \tilde{T}}{\partial x}+\tilde{v}\frac{\partial \tilde{T}}{\partial y}=\frac{k}{\rho c_p}\frac{\partial^2 \tilde{T}}{\partial y^2}+\frac{\mu}{\rho c_p}\left(\frac{\partial \tilde{u}}{\partial y}\right)^2-\frac{k_0}{\rho c_p}\left[\frac{\partial \tilde{u}}{\partial x}\left(\frac{\partial \tilde{u}}{\partial y}\right)^2+\tilde{u}\frac{\partial \tilde{u}}{\partial y}\frac{\partial^2 \tilde{u}}{\partial x\partial y}+\tilde{v}\frac{\partial \tilde{u}}{\partial y}\frac{\partial^2 \tilde{u}}{\partial y^2}+2\left(\frac{\partial \tilde{u}}{\partial y}\right)^2\frac{\partial \tilde{v}}{\partial y}\right]$$
$$+\frac{1}{\rho c_p}\frac{16\sigma^*\tilde{T}_\infty^3}{3k^*}\frac{\partial^2 \tilde{T}}{\partial y^2}+\frac{Q_0}{\rho c_p}(\tilde{T}-\tilde{T}_\infty)+\tau\left[D_B\frac{\partial \tilde{T}}{\partial y}\frac{\partial C}{\partial y}+\frac{D_{\tilde{T}}}{\tilde{T}_\infty}\left(\frac{\partial \tilde{T}}{\partial y}\right)^2\right], \tag{3}$$

$$\tilde{u}\frac{\partial \tilde{C}}{\partial x}+\tilde{v}\frac{\partial \tilde{C}}{\partial y}=D_B\left(\frac{\partial^2 \tilde{C}}{\partial y^2}\right)+\frac{D_{\tilde{T}}}{\tilde{T}_\infty}\left(\frac{\partial^2 \tilde{T}}{\partial y^2}\right)-K_r^2(\tilde{C}-\tilde{C}_\infty)\left[\frac{\tilde{T}}{\tilde{T}_\infty}\right]^n\exp\left[\frac{-E_a}{k_1\tilde{T}}\right], \tag{4}$$

Subject to the conditions

$$\begin{aligned}&\tilde{u}=U_w=ax,\ \tilde{v}=0,\ \tilde{T}=\tilde{T}_w,\ \tilde{C}=\tilde{C}_w \quad \text{at } y=0\\ &\tilde{u}\to 0,\ \tilde{T}\to\tilde{T}_\infty \quad \tilde{C}\to\tilde{C}_\infty \quad \text{as } y\to\infty\end{aligned} \tag{5}$$

Here (u,v) are velocity components in (x,y) directions, (k_0), (k), (c_p), (ρ), $(\tilde{\sigma})$, (σ^*), (k^*), (Q_0), (D_B), (K_r), (E_a), (k_1), and $(D_{\tilde{T}})$ denote material constant, density, electrical conductivity, specific heat, thermal conductivity, Stefan-Boltzmann constant, mean absorption coefficient, heat generation coefficient, Brownian diffusion coefficient, Boltzmann constant, dimensionless constant or rate constant having the range $-1<n<1$, chemical reaction parameter, activation energy and thermophoretic diffusion coefficient.

Considering

$$\psi=\sqrt{a\upsilon}x\,\hat{f}(\eta),\qquad \eta=\sqrt{\frac{a}{\upsilon}}y$$
$$\hat{\theta}(\eta)=\frac{\tilde{T}-\tilde{T}_\infty}{\tilde{T}_w-\tilde{T}_\infty},\qquad \hat{\phi}(\eta)=\frac{\tilde{C}-\tilde{C}_\infty}{\tilde{C}_w-\tilde{C}_\infty}. \tag{6}$$

Employing these transformation gives,

$$\hat{f}'''-\hat{f}'^2+\hat{f}\hat{f}''-K_0(2\hat{f}'\hat{f}''''-\hat{f}\hat{f}''''-\hat{f}''^2)-M\hat{f}'=0, \tag{7}$$

$$(1+R)\hat{\theta}''+\Pr Ec[K_0\hat{f}\hat{f}''\hat{f}'''+(\hat{f}'')^2]+\Pr N_b\hat{\theta}'\hat{\phi}'+\Pr N_t(\hat{\theta}')^2+\Pr\tilde{Q}\hat{\theta}=0, \tag{8}$$

$$\hat{\phi}''+\frac{N_t}{N_b}\hat{\theta}''+\Pr Le\,\hat{f}\hat{\phi}'-\Pr Le\tilde{A}^2(1+\tilde{\delta}\hat{\theta})^n\exp\left[\frac{-\dot{E}}{1+\tilde{\delta}\hat{\theta}}\right]\hat{\phi}=0, \tag{9}$$

$$\begin{aligned}&\hat{f}'(\eta)=1,\quad \hat{f}(\eta)=0\quad \hat{\theta}(\eta)=1,\quad \hat{\phi}(\eta)=1 \ \text{ at } \eta=0,\\ &\hat{f}'(\eta)\to 0,\quad \hat{\theta}(\eta)\to 0,\quad \hat{\phi}(\eta)\to 0 \quad \text{at } \eta\to\infty.\end{aligned} \tag{10}$$

where

$$K_0=\frac{k_0 a}{\mu},\quad M=\frac{\tilde{\sigma}B_0^2}{\rho a},\quad R=\frac{16\sigma^*\tilde{T}_\infty^3}{3kk^*},\quad \Pr=\frac{\mu c_p}{k},\quad Ec=\frac{U_w^2}{c_p(T_w-T_\infty)},$$

$$N_b=\frac{(\rho c)_p D_B(C_w-C_\infty)}{\upsilon(\rho c)_f},\quad N_t=\frac{(\rho c)_p D_T(T_w-T_\infty)}{\upsilon(\rho c)_f},\quad \tilde{Q}=\frac{Q_0}{a\rho c_p},\quad Le=\frac{(k/\rho c_p)}{D_B},\quad (11)$$

$$\overset{\circ}{E}=\frac{-E_a}{k_1\tilde{T}_\infty},\qquad \tilde{\delta}=\frac{(\tilde{T}_w-\tilde{T}_\infty)}{\tilde{T}_\infty},\qquad \tilde{A}=\frac{K_r^2}{a}.$$

In above expressions the definitions (M), $(\Pr)$, (N_t), (Le), (R), (Ec), $(\tilde{Q})$, (N_b), (K_0),$(\overset{\circ}{E})$, $(\tilde{\delta})$ and $(\tilde{A})$ denote magnetic parameter, Prandtl number, thermophoresis parameter, Lewis number, radiation parameter, Eckert number, heat generation variable, Brownian motion parameter, non-dimensional fluid parameter, dimensionless activation energy parameter, temperature ratio parameter and non-dimensional chemical reaction parameter respectively.
Coefficient of skin friction and Nusselt and Sherwood numbers are represented in to definitions given below

$$\tilde{C}_{fx}=\frac{2\tilde{\tau}_w\big|_{y=0}}{\rho U_w^2},\qquad (12)$$

$$\tilde{N}_{ux}=\frac{x\tilde{q}_w\big|_{y=0}}{k(\tilde{T}_w-\tilde{T}_\infty)},\qquad (13)$$

$$\tilde{S}_{hx}=\frac{x\tilde{q}_m\big|_{y=0}}{D_B(\tilde{C}_w-\tilde{C}_\infty)}.\qquad (14)$$

where

$$\tilde{\tau}_w=\mu\frac{\partial u}{\partial y}-k_0\left(u\frac{\partial^2 u}{\partial x\partial y}-2\frac{\partial u}{\partial x}\frac{\partial u}{\partial y}\right),\qquad (15)$$

$$\tilde{q}_w=k\frac{\partial\tilde{T}}{\partial y}+\frac{16\sigma^*\tilde{T}_\infty^3}{3k^*}\frac{\partial\tilde{T}}{\partial y},\qquad (16)$$

$$\tilde{q}_m=D_B\frac{\partial\tilde{C}}{\partial y}.\qquad (17)$$

Equation (6) and (12)-(17) give

$$\mathrm{Re}_x^{0.5}\,\tilde{C}_{fx}=2[1+K_0\,\overset{\vee}{f}'(0)]\,\overset{\vee}{f}''(0),\qquad (18)$$

$$\mathrm{Re}_x^{-0.5}\,\tilde{N}_{ux}=-\left(1+\frac{4}{3}R\right)\overset{\vee}{\theta}'(0),\qquad (19)$$

$$\mathrm{Re}_x^{-0.5}\,\tilde{S}_{hx}=-\overset{\vee}{\phi}'(0),\qquad (20)$$

where $\mathrm{Re}_x=\frac{xU_w}{\upsilon}$ is the local Reynold's number.

3. Entropy generation examination

Irreversibility analysis for nanofluid flow of Walter's-B fluid with Arrhenius activation energy is done here. Thermal radiation, viscous dissipation and MHD effects are also implemented on entropy generation minimization. Dimensional form under these effects is for

$$\left.\begin{aligned}\tilde{S}_{gen}''' = &\underbrace{\frac{k}{\tilde{T}^2}\left[1+\frac{16\sigma^*\tilde{T}_\infty^3}{3kk^*}\right]\left(\frac{\partial\tilde{T}}{\partial y}\right)^2}_{\text{heat transfer irreversibility}} + \underbrace{\frac{1}{\tilde{T}}\tilde{\Phi}}_{\text{viscous dissipation irreversibility}} + \underbrace{\frac{\sigma B_0^2\tilde{u}^2}{\tilde{T}}}_{\text{Joule heating irreversibility}} \\ &+\underbrace{\frac{RD}{\tilde{C}_\infty}\left(\frac{\partial\tilde{C}}{\partial y}\right)^2+\frac{RD}{\tilde{T}_\infty}\left(\frac{\partial\tilde{T}}{\partial y}\right)\left(\frac{\partial\tilde{C}}{\partial y}\right)}_{\text{Diffusive irreversibility}}\end{aligned}\right\} \tag{21}$$

$$\tilde{\Phi} = k_0\left[\frac{\partial u}{\partial x}\left(\frac{\partial u}{\partial y}\right)^2 + u\frac{\partial u}{\partial y}\frac{\partial^2 u}{\partial x\partial y} + v\frac{\partial u}{\partial y}\frac{\partial^2 u}{\partial y^2} + 2\left(\frac{\partial u}{\partial y}\right)^2\frac{\partial v}{\partial y}\right], \tag{22}$$

By substituting Eq. (22) into Eq. (21)

$$\left.\begin{aligned}\tilde{S}_{gen}''' = &\underbrace{\frac{k}{\tilde{T}^2}\left[1+\frac{16\sigma^*\tilde{T}_\infty^3}{3kk^*}\right]\left(\frac{\partial\tilde{T}}{\partial y}\right)^2}_{\text{heat transfer irreversibility}} + \underbrace{\frac{k_0}{\tilde{T}}\left[\frac{\partial u}{\partial x}\left(\frac{\partial u}{\partial y}\right)^2 + u\frac{\partial u}{\partial y}\frac{\partial^2 u}{\partial x\partial y} + v\frac{\partial u}{\partial y}\frac{\partial^2 u}{\partial y^2} + 2\left(\frac{\partial u}{\partial y}\right)^2\frac{\partial v}{\partial y}\right]}_{\text{viscous dissipation irreversibility}} \\ &+\underbrace{\frac{RD}{\tilde{C}_\infty}\left(\frac{\partial\tilde{C}}{\partial y}\right)^2+\frac{RD}{\tilde{T}_\infty}\left(\frac{\partial\tilde{T}}{\partial y}\right)\left(\frac{\partial\tilde{C}}{\partial y}\right)}_{\text{Diffusive irreversibility}} + \underbrace{\frac{\sigma B_0^2\tilde{u}^2}{\tilde{T}}.}_{\text{Joule heating irreversibility}}\end{aligned}\right\} \tag{23}$$

Employing transformations, entropy minimization becomes

$$\begin{aligned}N_G = &(1+R)\,\mathrm{Re}\,\overset{\vee}{\theta}'^2 + \frac{K_0 Br\,\mathrm{Re}}{\Omega_1}\overset{\vee}{f}\,\overset{\vee}{f}''\,\overset{\vee}{f}''' + \mathrm{Re}\,\lambda_1\left(\frac{\xi}{\Omega_1}\right)^2\overset{\vee}{\phi}'^2 \\ &+\mathrm{Re}\,\lambda\frac{\xi}{\Omega_1}\overset{\vee}{\theta}'\overset{\vee}{\phi}' + \frac{\mathrm{Re}\,MBr}{\Omega_1}\overset{\vee}{f}'^2,\end{aligned} \tag{24}$$

$$Br = \frac{\mu U_w^2}{k\Delta\tilde{T}}, \quad \Omega_1 = \frac{\Delta\tilde{T}}{\tilde{T}_\infty}, \quad \lambda_1 = \frac{RD\tilde{C}_\infty}{k}, \quad \xi = \frac{\Delta\tilde{C}}{\tilde{C}_\infty}$$

$$N_G = \frac{S_G'''\tilde{T}_\infty x^2}{k\left(\Delta\tilde{T}\right)^2}, \tag{25}$$

where (N_G), (λ_1), (Br), (ξ) and (Ω_1) denote total entropy rate, diffusion constant, Brinkman number,concentration and temperature difference parameters respectively.

4. Solution methodology

Series solution of above mentioned system is obtained via homotopic technique. The suitable initial iterations $(\overset{\vee}{f}_0, \overset{\vee}{\theta}_0, \overset{\vee}{\phi}_0)$ and corresponding linear operators $(\tilde{\pounds}_{\overset{\vee}{f}}, \tilde{\pounds}_{\overset{\vee}{\theta}}, \tilde{\pounds}_{\overset{\vee}{\phi}})$ are

$$\begin{aligned}\overset{\vee}{f}_0(\eta) &= 1 - e^{\eta}, \\ \overset{\vee}{\theta}_0(\eta) &= e^{-\eta}, \\ \overset{\vee}{\phi}_0(\eta) &= e^{-\eta},\end{aligned} \tag{26}$$

$$\tilde{\pounds}_{\overset{\vee}{f}}(\eta) = \frac{d^3\overset{\vee}{f}}{d\eta^3} - \frac{d\overset{\vee}{f}}{d\eta}, \quad \tilde{\pounds}_{\overset{\vee}{\theta}}(\eta) = \frac{d^2\overset{\vee}{\theta}}{d\eta^2} - \overset{\vee}{\theta}, \quad \tilde{\pounds}_{\overset{\vee}{\phi}}(\eta) = \frac{d^2\overset{\vee}{\phi}}{d\eta^2} - \overset{\vee}{\phi}, \tag{27}$$

$$\tilde{\pounds}_{\overset{\vee}{f}}\left[\hat{X}_1 + \hat{X}_2 e^{\eta} + \hat{X}_3 e^{-\eta}\right] = 0, \tag{28}$$

$$\tilde{\pounds}_{\theta}\left[\hat{X}_4 e^{\eta} + \hat{X}_5 e^{-\eta}\right] = 0, \tag{29}$$

$$\tilde{\pounds}_{\phi}\left[\hat{X}_6 e^{\eta} + \hat{X}_7 e^{-\eta}\right] = 0. \tag{30}$$

With $\hat{X}_i$ $(i = 1-7)$ are termed as arbitrary constants.

5. Convergence analysis

For this purpose the $\hbar$-curves are displayed in Fig. 2. It is noticed that series solutions converge for the ranges of auxiliary parameters satisfying $-1.5 \le \hbar_f \le -0.5$, $-1.4 \le \hbar_\theta \le -0.6$, and $-1.8 \le \hbar_\varphi \le -0.4$. Numerical values of convergent solution are displayed in Table 1. Clearly the momentum equation converges at 9^{th} order of approximation while 15^{th} and 19^{th} orders of approximations are enough for temperature and concentration. Comparison of reduced Nusselt number $(\mathrm{Re}_x^{-0.5}\,\tilde{N}_{ux})$ with published result are given in Table 2.

Figure 2
Table 1
Table 2

6. Discussion

Figs. (3-20) illustrates the velocity, temperature, concentration and entropy generation minimization in view of involved parameters. Fig. 3 presents outcome of (M) on velocity. For $(M = 0.1, 0.3, 0.5, 0.7)$ the velocity decays gradually when Lorentz fore (opposing force) enhances. In Fig. 4, change in velocity is shown for higher values of dimensionless fluid parameter (K_0). An increase in $(K_0 = 0.5, 0.6, 0.7, 0.8)$ yields reduction of velocity. Temperature for (N_t) variation is shown in Fig. 5. Temperature enhances for $(N_t = 0.5, 1, 1.4, 2.1)$. As heat transfer occurs from region of hotter region to the cooler part. This process boosts the temperature. Variation of (Pr) on temperature is shown in Fig. 6. Thermal diffusivity decays for $(\mathrm{Pr} = 1.1, 1.6, 2.2, 2.6)$ and so temperature reduces. Fig. 7 displays the outcome of Eckert number (Ec) on temperature. Temperature is an increasing function of $(Ec = 0.5, 0.9, 1.3, 1.6)$. Higher Eckert number give rise to kinetic energy of fluid and consequently fluid temperature enhances. Fig. 8 provides description of radiation on temperature. An increase of $(R = 0.2, 0.4, 0.6, 0.8)$ enhances temperature. Here radiation parameter defines the transfer rate of thermal radiation relative to conductive heat transfer rate. For higher values of radiation parameter the radiation term dominates over conduction. Hence more heat releases in a system due to radiative heat flux and so temperature increases. Fig. 9 gives outcome of $(\tilde{Q})$ on temperature. Temperature increases as $(\tilde{Q} = 0.1, 1, 1.7, 2.4)$ generates energy in system. Outcomes of (N_t) and (N_b) on concentration are sketched in Figs. 10 and 11. Opposite trend are observed in case of higher $(N_t = 0.5, 0.9, 1.3, 1.7)$ and $(N_b = 0.6, 0.9, 1.6, 2.7)$ for concentration. Variation in fluids concentration against dimensionless chemical reaction parameter $(\tilde{A})$ is pictured in Fig. 12 Increasing $(\tilde{A} = 0.5, 0.9, 1.25, 1.55)$ lead to reduction of concentration. Fig. 13 provides impact of activation energy parameter $(\overset{\circ}{E})$ on concentration. It can be seen through figure that concentration rises for higher $(\overset{\circ}{E} = 0.2, 1.5, 2.1, 2.9)$.

Figure 3
Figure 4
Figure 5
Figure 6
Figure 7
Figure 8
Figure 9
Figure 10
Figure 11
Figure 12
Figure 13

Influences of M and K_0 on $\mathrm{Re}_x^{0.5}\tilde{C}_{fx}$ are disclosed in Fig. 14. It is clear that $\mathrm{Re}_x^{0.5}\tilde{C}_{fx}$ increases for higher M and K_0. Fig. 15 depicts the effects of Ec and R on $\mathrm{Re}_x^{-0.5}\tilde{N}_{ux}$. Higher values of R and Ec decay $\mathrm{Re}_x^{-0.5}\tilde{N}_{ux}$. Variations of $\overset{\circ}{E}$ and σ on $\mathrm{Re}_x^{-0.5}\tilde{S}_{hx}$ are shown in Fig. 16. $(\mathrm{Re}_x^{-0.5}\tilde{S}_{hx})$ is decreasing function of $\overset{\circ}{E}$ and $\tilde{A}$.

Figure 14
Figure 15
Figure 16

7. Entropy rate analysis

Fig. 17 elucidates the outcome of M on $N_G(\eta)$. Clearly $N_G(\eta)$ increases for larger M. Consequences of Brinkman number Br on $N_G(\eta)$ are disclosed in Fig. 18. $N_G(\eta)$ enhances by higher Br. Infact irreversibility occurs in fluid friction by higher Br. Fig. 19 indicates effectiveness of K_0 on $N_G(\eta)$. An increase in $N_G(\eta)$ is noticed for K_0. Figs. 20 presents influence of temperature difference parameter ξ on $N_G(\eta)$. For higher ξ the entropy generation minimization increases. It is because of the fact that the heat transfer dominates in comparison to fluid friction and magnetic field for higher ξ.

Figure 17
Figure 18
Figure 19
Figure 20

8. Conclusions

Radiative nanofluid flow of Walters-B fluid under the effect of activation energy is investigated analytically. Significance of entropy rate and heat/generation absorption on assumed simulations are observed and debated graphically. Remarkable highlights can be concluded as:

- Qualitative effect of concentration and temperature are reversed for higher thermophoresis parameter.
- Temperature has similar behavior for radiation and Eckert number.
- An enhancement of temperature is possible for heat/generation parameter.
- Concentration by an activation energy parameter is increased.
- Decrease in mass transfer rate is noticed.
- Opposite behavior of total entropy rate for fluid parameter and temperature difference

parameter are noticed.

- Total entropy rate is an increasing function of Brinkman number and magnetic parameter.

References

1. Choi, S. U. S. ‘‘Enhancing Thermal Conductivity of Fluids With Nanoparticles’’, ASME-Publications-Fed, 231, pp. 99-106 (1995).
2. Waini, I. Ishak, A. and Pop, I. ‘‘Hybrid nanofluid flow and heat transfer over a nonlinear permeable stretching/shrinking surface’’, Int. J. Numerical Meth. Heat & Fluid Flow, (2019) 0057
3. Sheikholeslami, M. ‘‘Numerical approach for MHD Al_2O_3-water nanofluid transportation inside a permeable medium using innovative computer method’’, Comp. Meth. Appl. Mech. Eng. 344, pp. 306-318 (2019)
4. Aly E. H., ‘‘Dual exact solutions of graphene--water nanofluid flow over stretching/shrinking sheet with suction/injection and heat source/sink: Critical values and regions with stability’’, Powder Tech. 342 pp. 528-544 (2019)
5. Rafiq, T. Mustafa, M. and Khan J. A., ‘‘Numerical study of Bödewadt slip flow on a convectively heated porous disk in a nanofluid’’, Phys. Scr. (2019) ab1549.
6. Hsiao, K. L. ‘‘Micropolar nanofluid flow with MHD and viscous dissipation effects towards a stretching sheet with multimedia feature’’, Int. J. Heat and Mass Transf., 112, pp. 983—990 (2017).
7. Turkyilmazoglu, M. ‘‘MHD natural convection in saturated porous media with heat generation/absorption and thermal radiation: closed-form solutions’’, Archi. Mech., 71, pp. 49-64 (2019).
8. Ramzan, M. Bilal, M. and Chung, J. D. ‘‘Effects of thermal and solutal stratification on jeffrey magneto-nanofluid along an inclined stretching cylinder with thermal radiation and heat generation/absorption’’, Int. J. Mech. Sci., 132, pp. 317-324 (2017).
9. Hsiao, K. L. ‘‘To promote radiation electrical MHD activation energy thermal extrusion manufacturing system efficiency by using Carreau-nanofluid with parameters control method’’, Energy, 130 (2017) 486-499
10. Mustafa, M. Khan, J. A. Hayat, T. et al. ‘‘Buoyancy effects on the MHD nanofluid flow past a vertical surface with chemical reaction and activation energy’’, Int. J. Heat and Mass Transf. 108, pp. 1340-1346 (2017).
11. Hsiao, K. L. ‘‘Stagnation electrical MHD nanofluid mixed convection with slip boundary on a stretching sheet’’, Appl. Therm. Eng., 98, pp. 850--861(2016).
12. Bejan, A. “A study of entropy generation in fundamental convective heat transfer”, ASME J. Heat Transfer, 101 (4), pp. 718-725 (1979).
13. Bejan, A. Kestin, J. “Entropy generation through heat and fluid flow”, J. Appl. Mech., 50 (1983).
14. Liu, Y. Jian, Y. and Tan, W. “Entropy generation of electromagnetohydrodynamic (EMHD) flow in a curved rectangular microchannel”, Int. J. Heat Mass Transf., 127, pp. 901-913 (2018).
15. Qayyum. S. Khan, M. I. Hayat, T. et al., “Entropy generation in dissipative flow of Williamson fluid between two rotating disks”, Int. J. Heat Mass and Transf., 127,pp. 933-942 (2018).
16. Akbarzadeh, M. Rashidi, S. Karimi, N. “Convection of heat and thermodynamic irreversibilities in two-phase, turbulent nanofluid flows in solar heaters by corrugated absorber plates”, Adv. Powder Techn., 29, pp. 2243-2254 (2018).

17. Bizhaem, H. K. Abbassi, A. "Numerical study on heat transfer and entropy generation of developing laminar nanofluid flow in helical tube using two-phase mixture model", Adv. Powder Techn., 28 (9) pp. 2110-2125 (2017).
18. Pal, S. K. Bhattacharyya, S. and Pop, I. "Effect of solid-to-fluid conductivity ratio on mixed convection and entropy generation of a nanofluid in a lid-driven enclosure with a thick wavy wall", Int. J. Heat and Mass Transf., 127, pp. 885-900 (2018).
19. Sheikholeslami, M. Ganji, D.D. "Entropy generation of nanofluid in presence of magnetic field using lattice Boltzmann method", Physica A, 417, pp. 273-286 (2015).
20. Wang, Y. Chen, Z. and Ling, X., "Entropy generation analysis of particle suspension induced by Couette flow," Int. J. Heat Mass Transf., 90 pp. 499-504 (2015).
21. Hayat, T. Khan, M. I. Qayyum, S. et al., "Entropy generation for flow of Sisko fluid due to rotating disk", J. Mol. Liq., 264, pp. 375-385 (2018).
22. Liao, S. J. "Homotopy analysis method in non-linear differential equations" (Springer and Higher Education Press, Heidelberg, 2012).
23. Noeiaghdam, S. Zarei, E. and Kelishami, H. B. "Homotopy analysis transform method for solving Abel's integral equations of the first kind", Ain Shams Eng. J. 7. pp. 483-495 (2016).
24. Hayat, T. Mustafa, M. and Asghar, S. "Unsteady flow with heat and mass transfer of a third grade fluid over a stretching surface in the presence of chemical reaction", Nonlinear Analysis: Real World Appl. 11 (4), pp. 3186-3197 (2010).
25. Rahman, S. Hayat, T. Muneer, M. et al. "Global existence of solutions for MHD third grade flow equations saturating porous medium", Comput. Math. Appl., 76, pp. 2360-2374 (2018).
26. Jabeen, S. Hayat, T. Alsaedi, A. et al. "Consequences of activation energy and chemical reaction in radiative flow of tangent hyperbolic nanoliquid", Scientia Iranica, (2019) DOI: 10.24200/SCI.2019.52726.2860.
27. Imtiaz, M. Kiran, A. Hayat, T. et al. "Axisymmetric flow by a rotating disk with Cattaneo--Christov heat flux", J. Braz. Soc. Mec. Sci. Eng., 41, pp. 149 (2019).
28. Hayat, T. Ahmad, S. Khan, M. I et al. "Modeling and analyzing flow of third grade nanofluid due to rotating stretchable disk with chemical reaction and heat source", Physica B: Cond. Matt., 537, pp. 116-126 (2018).
29. Abbasbandy, S. Mustafa, M. "Analytical and numerical approaches for Falkner--Skan flow of MHD Maxwell fluid using a non-Fourier heat flux model", Int. J. Num. Meth. Heat & Fluid Flow, 28, pp.1539-1555 (2018).
30. Turkyilmazoglu, M. "Convergence accelerating in the homotopy analysis method: a new approach", Adv. Appl. Math. Mech., 10, pp. 1-24 (2018).
31. Hayat, T. Qayyum, S. Khan, M. I. et al. "Entropy generation in magnetohydrodynamic radiative flow due to rotating disk in presence of viscous dissipation and Joule heating", Phys. Fluids, 30 (2018) 017101.
32. Qayyum, S. Hayat, T. Jabeen, S. "Entropy generation in nanofluid flow of Walters-B fluid with homogeneous-heterogeneous reactions", Math. Meth. Appl. Sci. pp. 1—16 (2020).
33. Hsiao, K. L. "Combined electrical MHD heat transfer thermal extrusion system using Maxwell fluid with radiative and viscous dissipation effects", Appl. Therm. Eng., 112, pp. 1281-1288 (2017).
34. Turkyilmazoglu, M. "Multiple analytic solutions of heat and mass transfer of magnetohydrodynamic slip flow for two types of viscoelastic fluids Over a stretching

surface", J. Heat Transfer, 134(7), pp. 071701 (2012)
35. Turkyilmazoglu, M. "An effective approach for approximate analytical solutions of the damped Duffing equation", Phy. Scrip. 86(1), pp. 015301 (2012).

Figures and Tables:

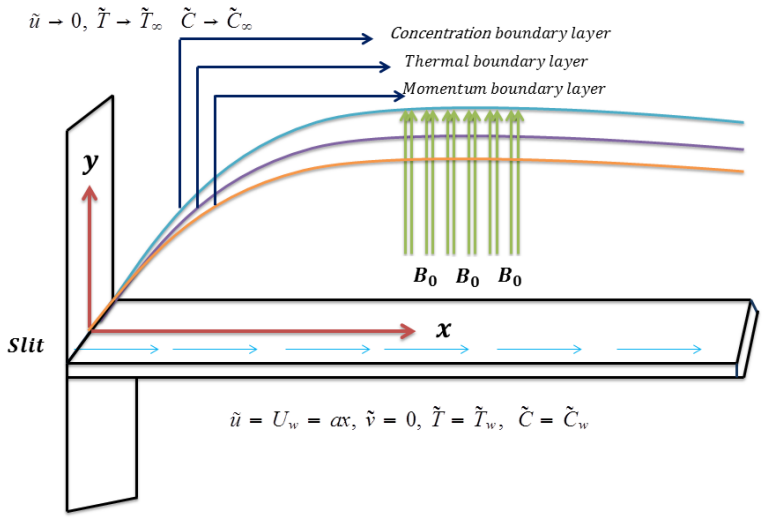

Fig. 1: Flow geometry

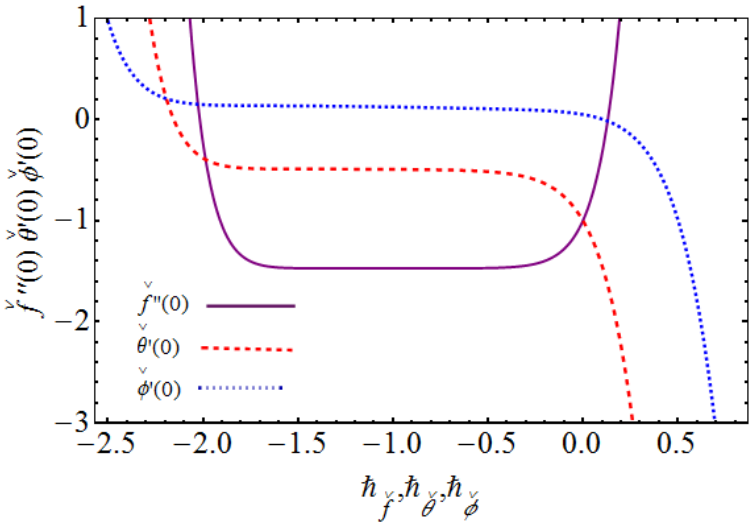

Fig. 2: $\hbar-$ curves for $\hbar_f, \hbar_\theta$ and $\hbar_\phi$.

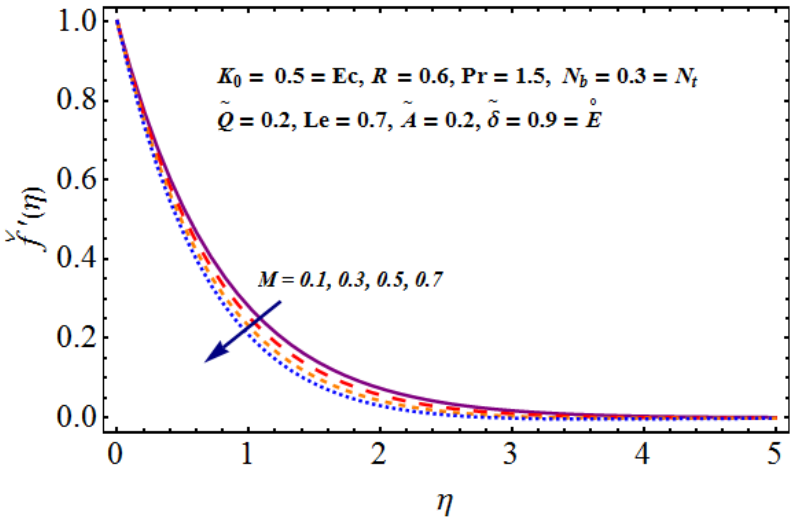

Fig. 3: Impact on $\check{f}(\eta)$ via M

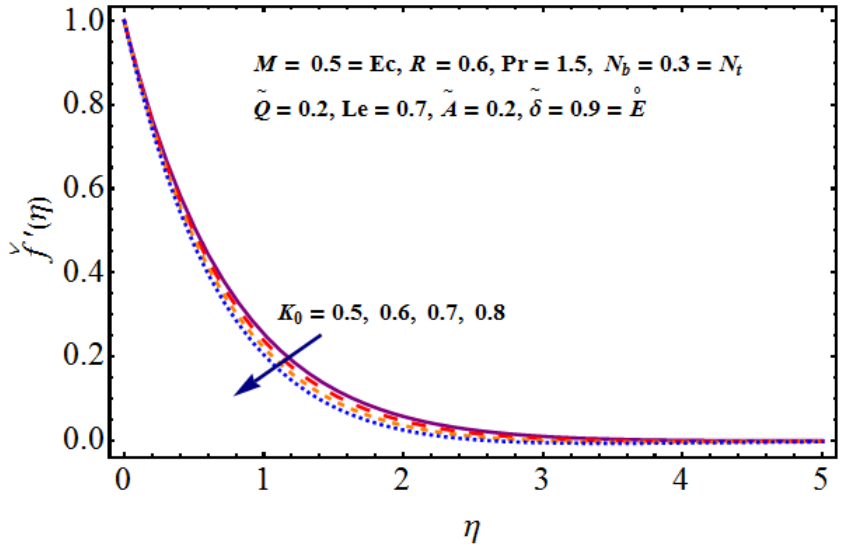

Fig. 4: Impact on $\breve{f}(\eta)$ via K_0

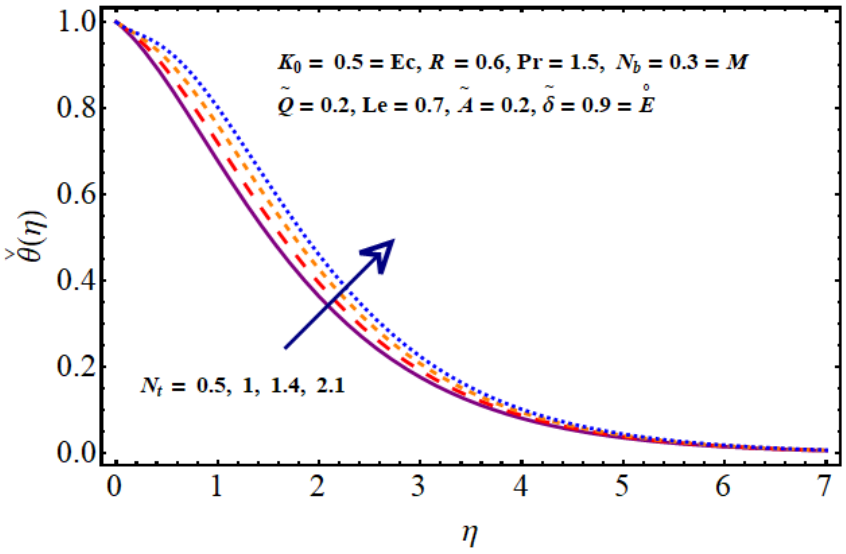

Fig. 5: Impact on $\breve{\theta}(\eta)$ via N_t

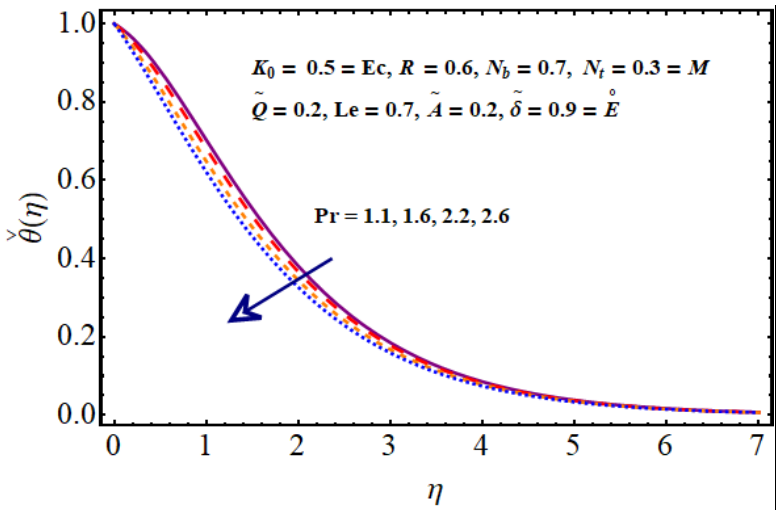

Fig. 6: Impact on $\breve{\theta}(\eta)$ via Pr

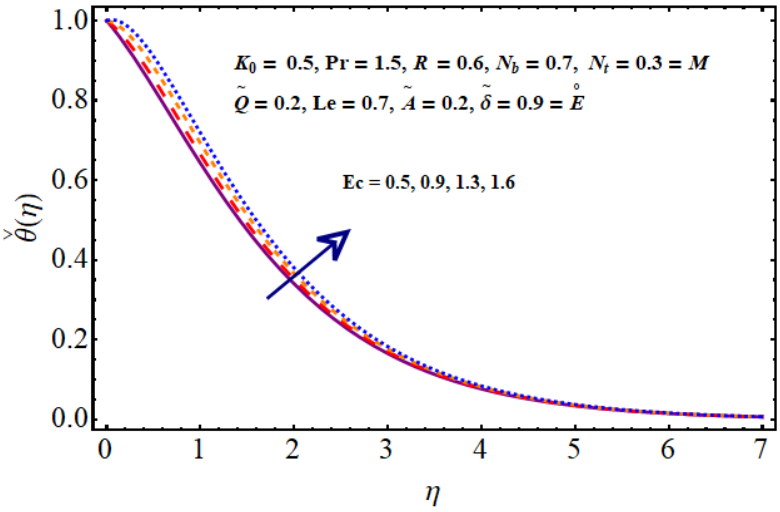

Fig. 7: Impact on $\breve{\theta}(\eta)$ via *Ec*

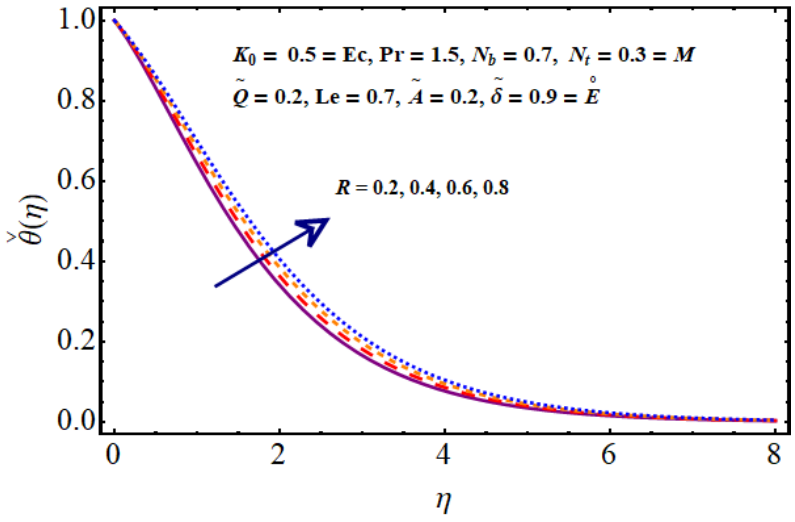

Fig. 8: Impact on $\breve{\theta}(\eta)$ via R

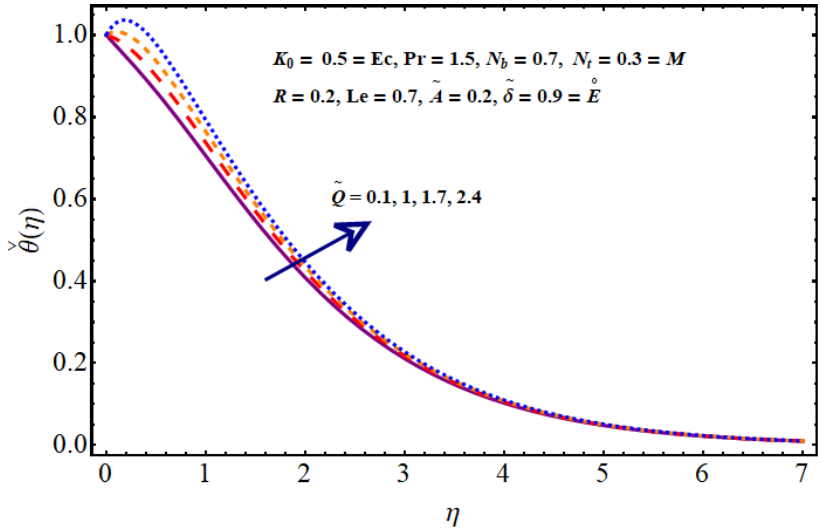

Fig. 9: Impact on $\breve{\theta}(\eta)$ via $\tilde{Q}$

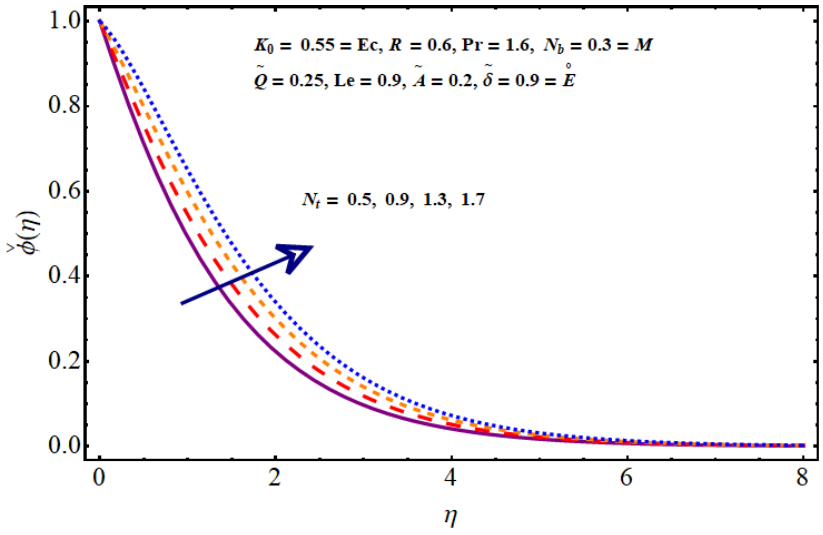

Fig. 10: Impact on $\check{\phi}(\eta)$ via N_t

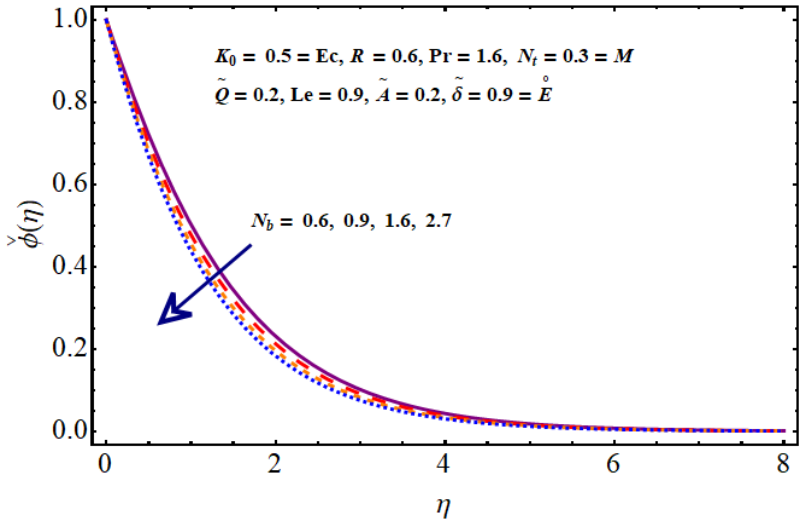

Fig. 11: Impact on $\check{\phi}(\eta)$ via N_b

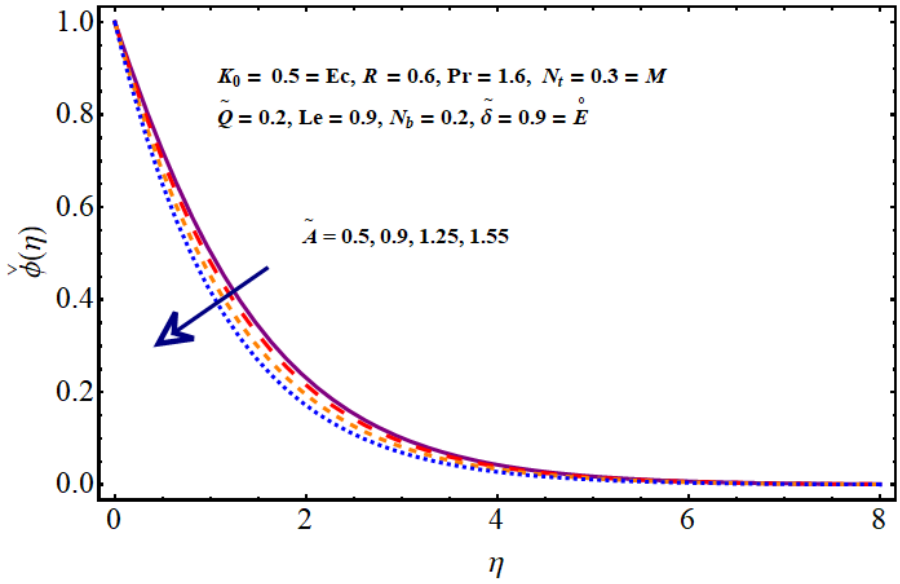

Fig. 12: Impact on $\breve{\phi}(\eta)$ via $\tilde{A}$

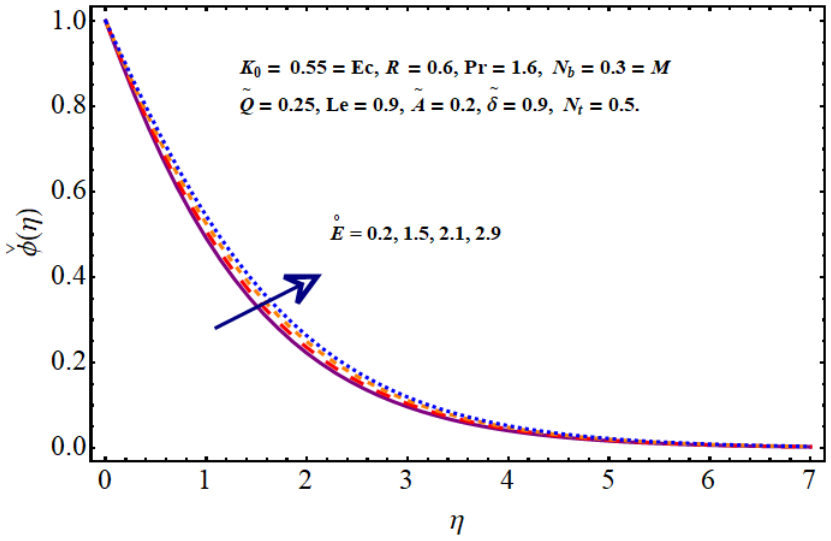

Fig. 13: Impact on $\breve{\phi}(\eta)$ via $\mathring{E}$

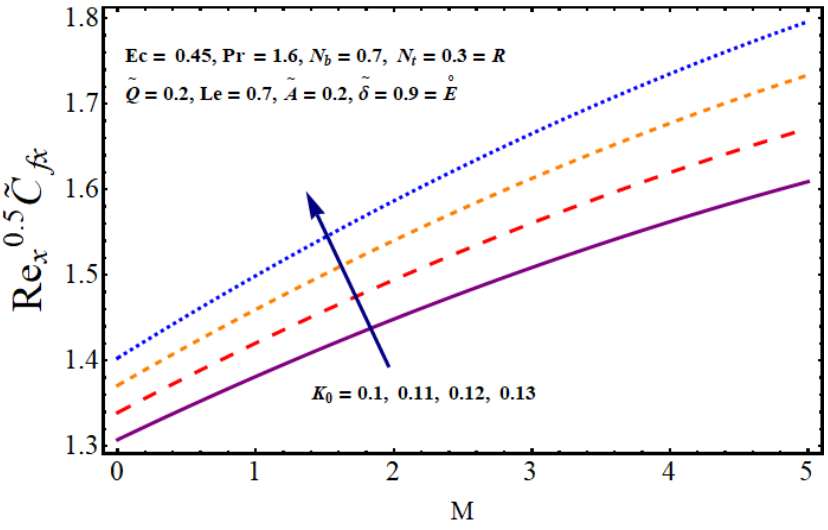

Fig. 14: Impact of M and K_0 on $\mathrm{Re}_x^{0.5}\tilde{C}_{fx}$.

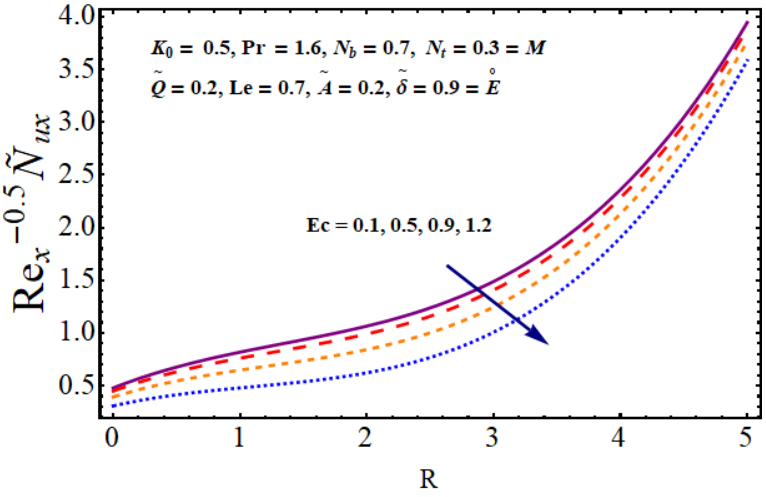

Fig. 15: Impact of R and Ec on $\mathrm{Re}_x^{-0.5}\tilde{N}_{ux}$.

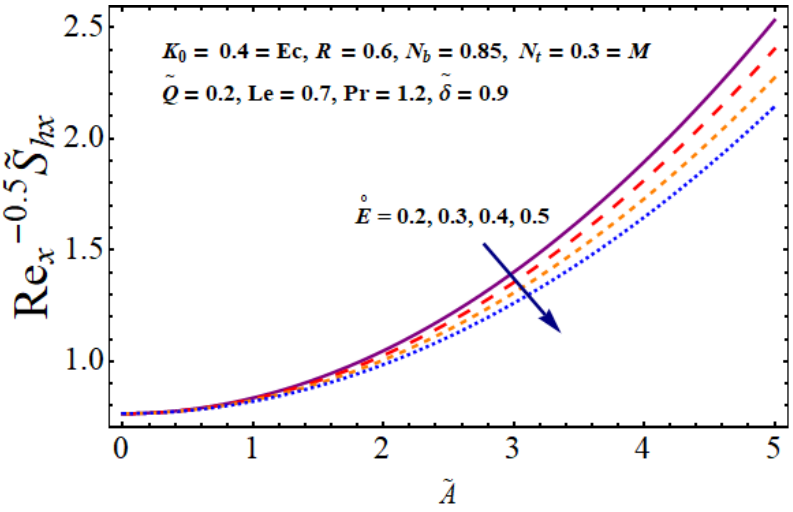

Fig. 16: Impact of $\tilde{A}$ and $\mathring{E}$ on $\mathrm{Re}_x^{-0.5}\tilde{S}_{hx}$.

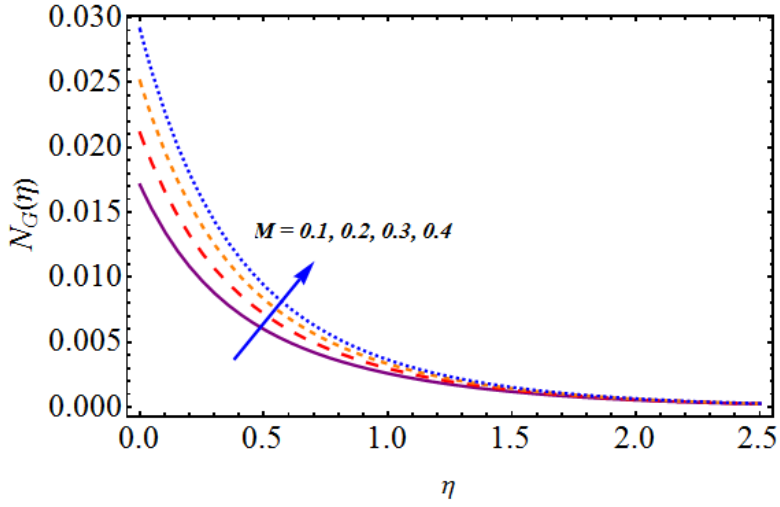

Fig. 17: Impact of M on N_G.

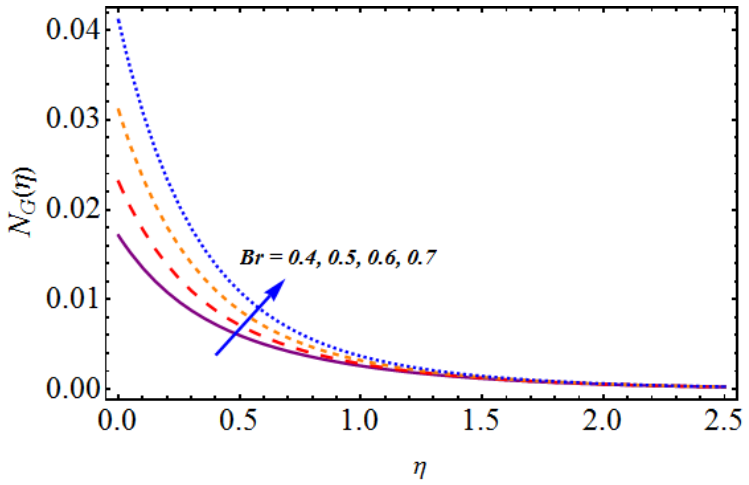

Fig. 18: Impact of Br on N_G.

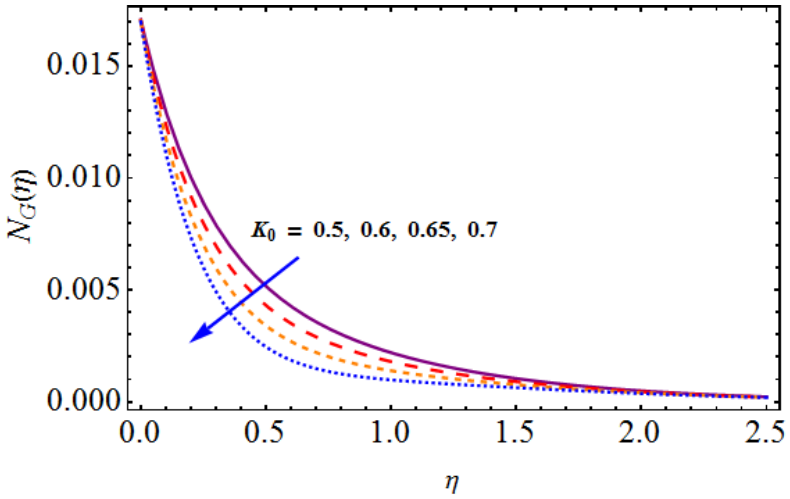

Fig. 19: Impact of K_0 on N_G

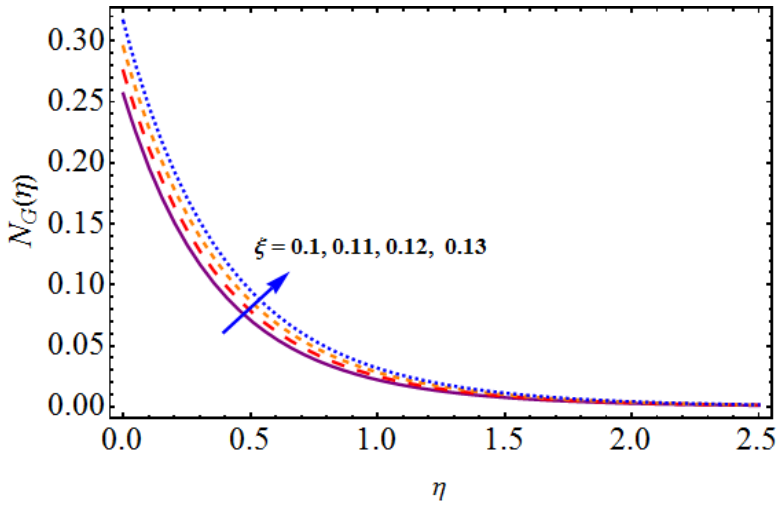

Fig. 20: Impact of ξ on N_G

Table 1: Convergence table for velocity, temperature and concentration when $M = 0.3,\ \Pr = 1.2\ N_t = 0.4 = Le, R = 0.7 = Ec,\ \widetilde{Q} = 0.3,\ N_b = 0.25 = K_0,\ \overset{\circ}{E} = 0.9 = \widetilde{\delta}$ and $\widetilde{A} = 0.65$

Order of approximations	$-\overset{\vee}{f}''(0)$	$-\overset{\vee}{\theta}'(0)$	$\overset{\vee}{\phi}'(0)$
1	1.3500	0.73167	0.077040
9	1.4719	0.49925	0.11297
15	1.4719	0.49195	0.12603
19	1.4719	0.49195	0.12967
30	1.4719	0.49195	0.12967
40	1.4719	0.49195	0.12967

Table 2: Code verification for $\mathrm{Re}_x^{-0.5}\,\tilde{N}_{ux}$ when , $R=0=K_0$ for values of $\overset{\circ}{E}$ and $\tilde{A}$.

$\overset{\circ}{E}$	$\tilde{A}$	Mustafa et al. [10]	Present
0	1	0.9412	0.9412
1		1.0139	1.0139
2		1.0645	1.0645
4		1.1145	1.1145
1	0	1.1453	1.1453
1	1	1.0139	1.0139
	2	0.9262	0.9262
	5	0.7986	0.7986

Biography of authors:

- **Sumaira Jabeen** is Ph.D student of mathematics at Quaid-i-Azam university, Pakistan. She received his master's degree from Quaid-i-Azam university. Her research interests are fluid mechanics, non-linear flow problems and heat transfer.
- **Tasawar Hayat** is a Pakistani mathematician who has made pioneering research contributions to the area of mathematical fluid mechanics. He is considered one of the leading mathematicians working in Pakistan and currently is a Professor of Mathematics at the Quaid-i-Azam University
- **Ahmad Alsaedi** is professor of department of mathematics at King Abdulaziz University, Jeddah ,Saudi Arabia. He belongs to Nonlinear Analysis and Applied Mathematics (NAAM) research group. His area of interests includes fluid dynamics, non linear flow analysis and flow problem in nanosystems.